

Supplementary Materials for

Proteomic and Functional Genomic Landscape of Receptor Tyrosine Kinase and Ras to Extracellular Signal–Regulated Kinase Signaling

Adam A. Friedman, George Tucker, Rohit Singh, Dong Yan, Arunachalam Vinayagam, Yanhui Hu, Richard Binari, Pengyu Hong, Xiaoyun Sun, Maura Porto, Svetlana Pacifico, Thilakam Murali, Russell L. Finley Jr., John M. Asara, Bonnie Berger, Norbert Perrimon*

*To whom correspondence should be addressed. E-mail: perrimon@receptor.med.harvard.edu

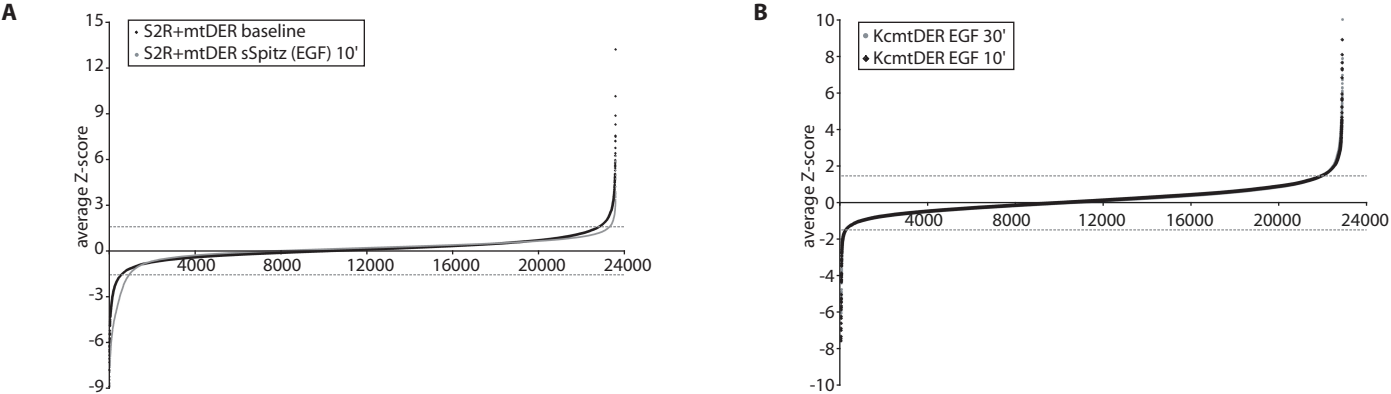
Published 25 October 2011, *Sci. Signal.* **4**, rs10 (2011)
DOI: 10.1126/scisignal.2002029

This PDF file includes:

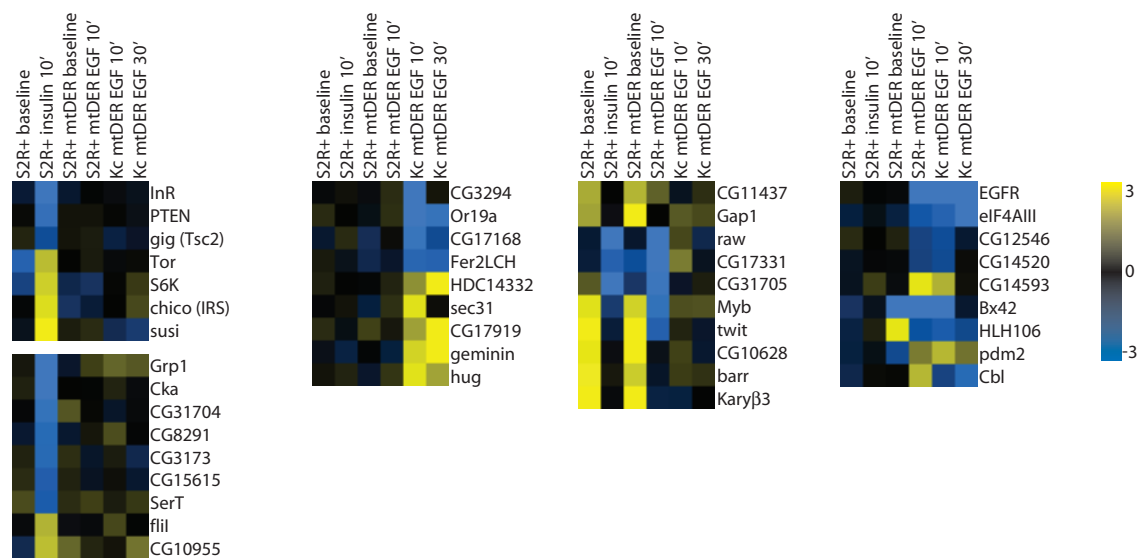
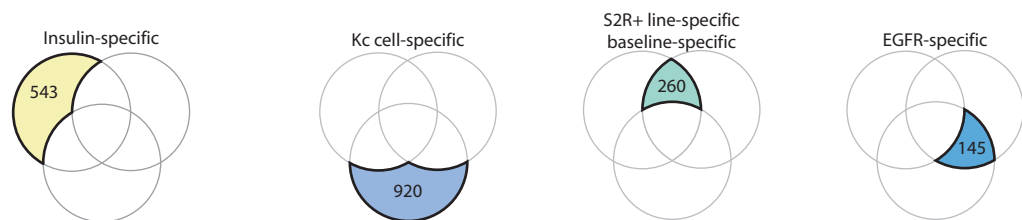
Fig. S1. Primary RNAi screen optimization and data.
Fig. S2. Performance of SAINT-based PPI ranking.
Fig. S3. Validation of additional PPI interactions.
Fig. S4. Phenotypes of additional RTK-Ras-ERK network components based on in vivo RNAi.
Table S3. RTK-specific hit subsets.

Other Supplementary Material for this manuscript includes the following: (available at www.sciencesignaling.org/cgi/content/full/4/196/rs10/DC1)

Table S1. Compilation of all hits from six genome-wide RNAi screens performed in duplicate, and grouping by screen type.
Table S2. Gene Ontology Biological Process and Molecular Function categories enriched in RNAi screen hits and PPI data.
Table S4. Protein-protein interactions determined by TAP-MS analysis of RTK-Ras-ERK canonical pathway.
Table S5. Compilation of all in vivo results.
Table S6. Hairpin lines used for in vivo analyses.
Cytoscape file for the PPI and RNAi data.
Excel spreadsheets of peptides isolated in each TAP-MS experiment.



C



D

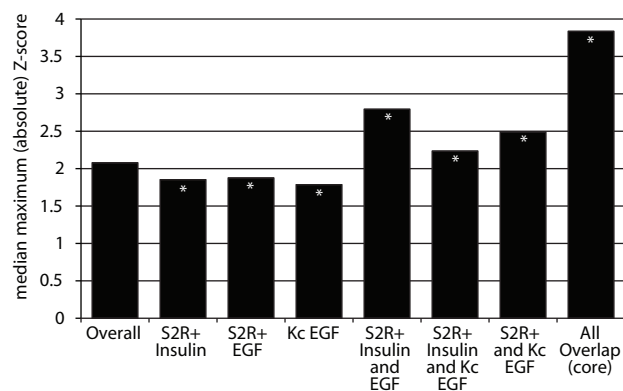


fig. S1. Primary RNAi screen optimization and data. (A) Profile of average Z-score for all dsRNAs screened, by condition, in the primary screen for RTK-Ras-ERK regulators downstream of EGFR activation in S2R+mtEGFR *Drosophila* cells. Baseline samples were not stimulated with sSpitz-conditioned medium. (B) Profile of average Z-score for all dsRNAs screened, by condition, in the primary screen for RTK-Ras-ERK regulators downstream of EGFR activation in Kc mtEGFR cells following 10 or 30 minutes of EGF stimulus. (C) Subgroups of RNAi screen hits based on appearance in overlapping primary RNAi screens. Genes appearing in distinct subsets may play context-specific roles. Primary RNAi data are shown, with the color of each box corresponding to the average Z-score according to the scale to the upper right. (D) Average maximum Z-score for genes in the given groups of individual or overlapping sets of genes from the three primary screen groups; in general, genes scoring in more than one screen group had higher Z-scores than all RNAi hits overall, reflecting either increased likelihood of scoring above assay noise, or that newly identified core pathway genes with higher scores are required in a context-independent manner. * denotes $p < 0.05$ by Mann-Whitney test.

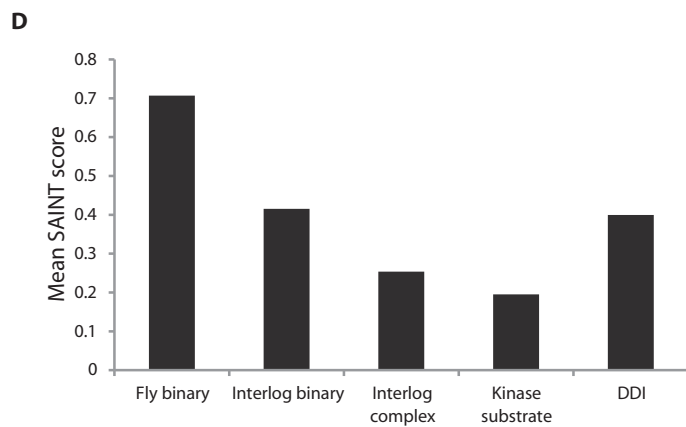
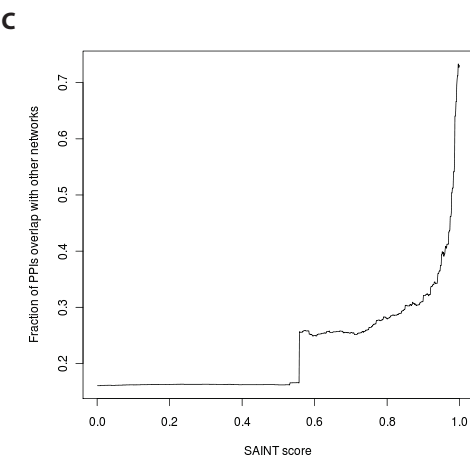
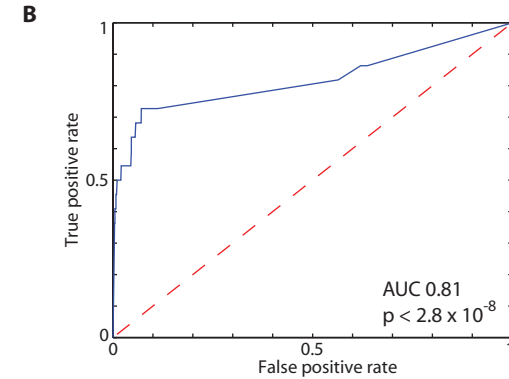
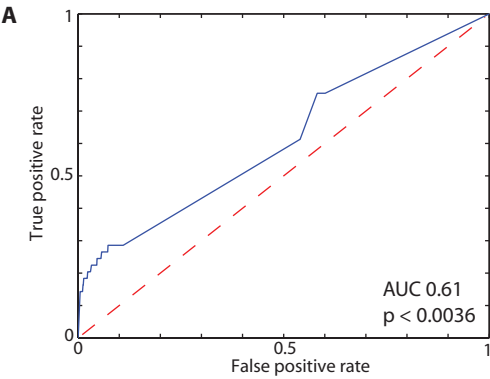


fig. S2. Performance of SAINT-based PPI ranking. (A) Receiver operating characteristic (ROC) curve for SAINT analysis based on BioGRID gold standard. Area under the curve was calculated as 0.6124, $p < 0.003$. (B) ROC for SAINT analysis based on fly features of MasterNet. Area under the curve was calculated as 0.8182, $p < 2.8 \times 10^{-8}$. (C) SAINT score accurately predicts literature-based validation of protein interactions. (D) Fly binary literature interactions more accurately predict higher SAINT scores. Networks are as described in MasterNet, see Materials and Methods. ROC p values were calculated using a normal distribution for the Wilcoxon rank-sum test (1).

1. S. J. Mason, N. E. Graham, Areas beneath the relative operating characteristics (ROC) and relative operating levels (ROL) curves: Statistical significance and interpretation. *Quarterly Journal of the Royal Meteorological Society* **128**, 2145 (2002).

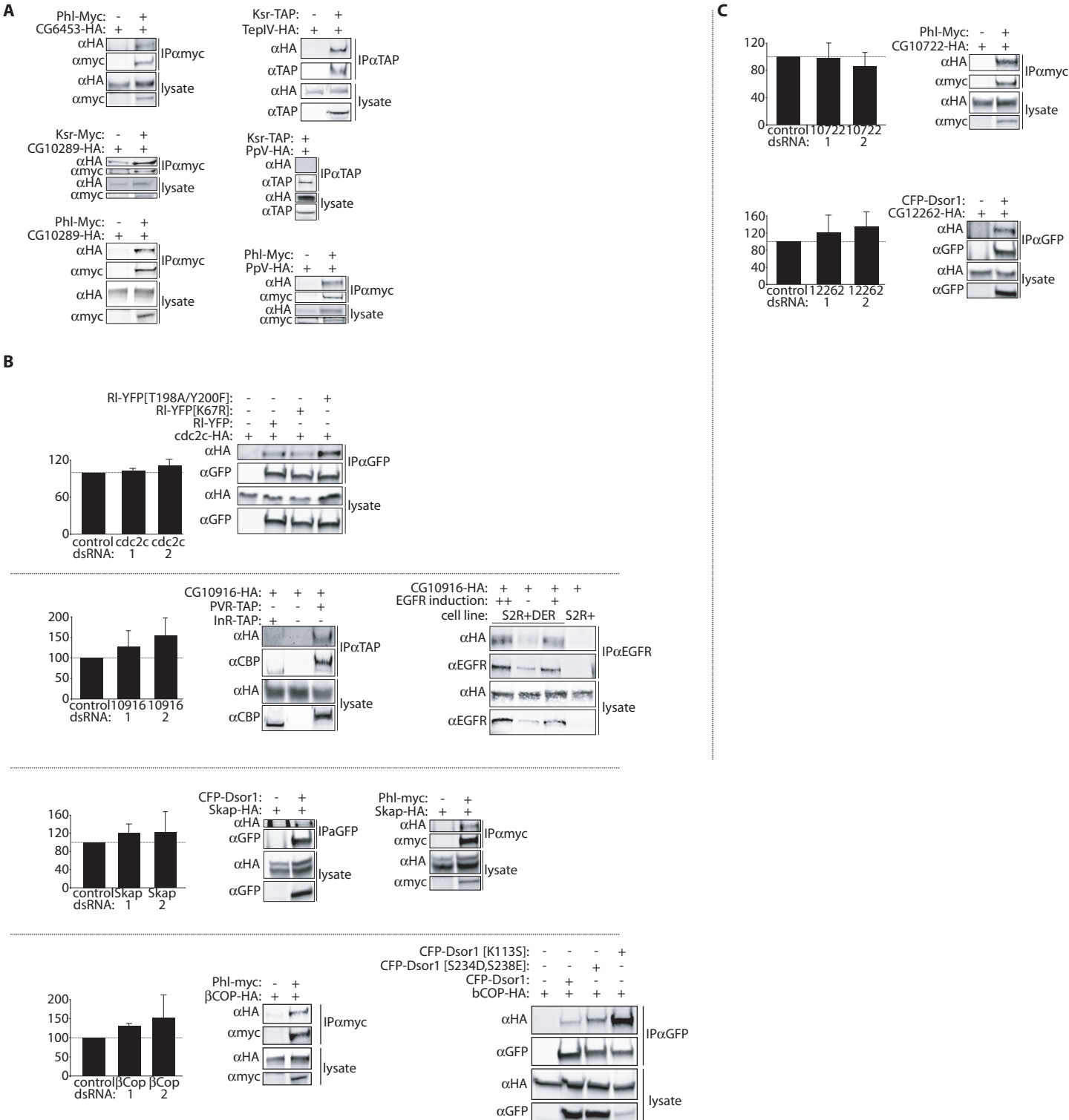
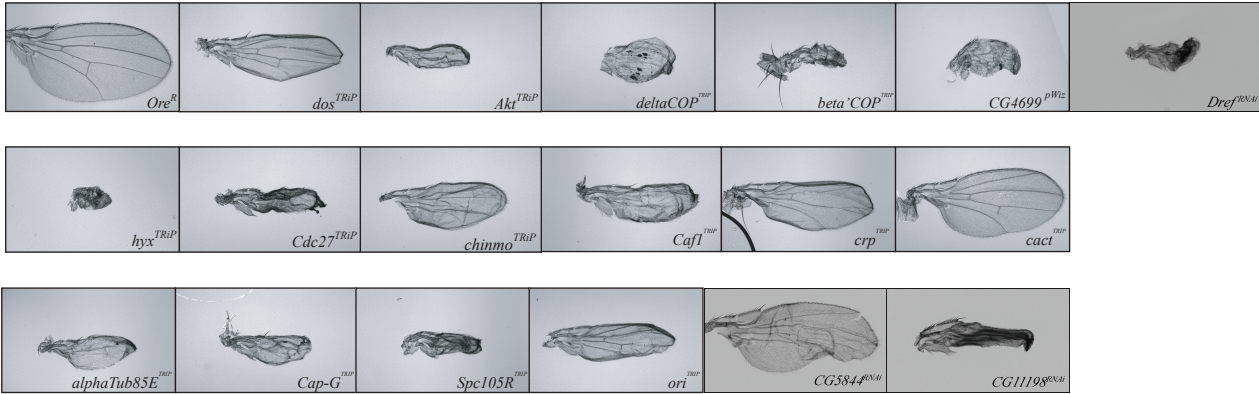


fig. S3. Validation of additional PPI interactions. (A) Coimmunoprecipitation (co-IP) experiments validating proteins studied in vivo and shown in Fig. 5. (B) The graphs shown display results of RNAi experiments towards the indicated genes. RNAi validation was performed using two independent dsRNAs per gene and quantitative Western blotting to dpERK normalized to total ERK in various conditions, expressed as percent of control dsRNA ERK activation (*CG10722*, insulin; *CG6453*, sSpitz (EGF); *Skap*, insulin; *betaCOP*, sSpitz (EGF); *CG12262*, insulin). Note Cdc2c binds ERK, an interaction not requiring kinase catalytic activity (K67R mutant) or activation (T198A, Y200F mutant). CG10196 binds all three RTKs (EGFR, InR, and PVR). A number of interactions filtered out by SAINT score < 0.83 were validated by co-IP, suggesting our SAINT cutoff is a conservative estimate of RTK-Ras-ERK interactors. For example, *Skap* interactions with Phl (Raf) were detected by co-IP, despite being excluded from our “filtered” network on the basis of SAINT score. Similarly, beta-COP interactions with Dsor1 (MEK) were filtered by SAINT score but verified by co-IP; both constitutively active (S234D, S238E) and dominant-negative (K113S) Dsor1 bound beta-COP more strongly than did wild-type Dsor1. That these proteins interact with other components of the same known complex (Phl-Dsor1 complex) suggests that the interactions excluded on the basis of SAINT score may in fact be real and specific. (C) Additional interactions with SAINT scores < 0.83 that were replicated in directed co-IP analysis include the interaction of CG10722 with Phl and of CG12262 with Dsor1. Antibodies used for Western blotting or coimmunoprecipitations are indicated as α and the name of the protein that the antibody recognizes, for example, α GFP means an antibody recognizing green fluorescent protein (GFP) and the GFP variant CFP. CBP is a component of the TAP tag; thus, the antibody called α CBP recognizes TAP fusion proteins.

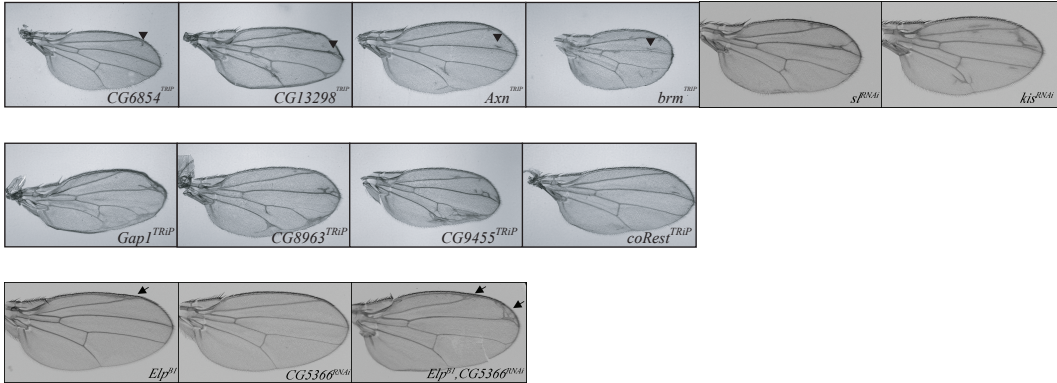
A

Positive regulators



B

Negative regulators



C

Enhancers of Ras^{N17}



Suppressors of Ras^{N17}



D

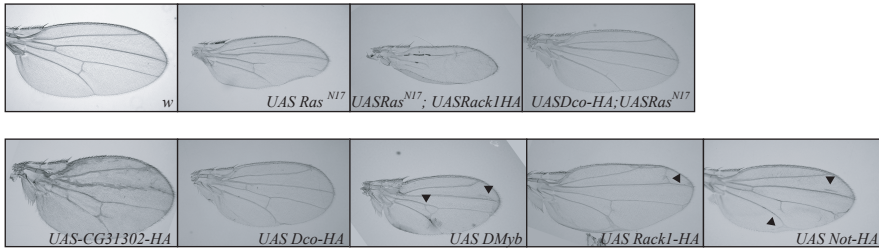


fig. S4. Phenotypes of additional RTK-Ras-ERK network components based on in vivo RNAi. (A) Phenotypes consistent with positive regulation of wing disc growth and survival, as compared to wild-type *Ore^R*. (B) Phenotypes consistent with negative regulation of wing disc RTK activity as evidenced by increased wing size or ectopic wing vein material. (C) Phenotypes of enhancement (top) or suppression (bottom) of the *Ras^{N17}* (a dominant-negative Ras transgene) phenotype of decreased wing size and characteristic missing section of L4 wing vein. (D) Top, enhancement or suppression phenotypes of overexpressing cDNAs for selected network components in background of *Ras^{N17}*; *w* control is shown for comparison. Bottom, isolated overexpression phenotypes consistent with positive regulation of the *Ras* pathway. For panels A through C, the RNAi transgene backbone used is indicated as an allele superscripted above the gene targeted, as described in Materials and Methods and table S6.

Friedman, Perrimon, et al., 2011
table S3: RTK-specific hit subsets

Friedman, Perrimon, <i>et al.</i> , 2011 table S3: RTK-specific hit subsets			MAPK Phenotype				Primary RNAi Screen Score						Human Disease	Human Ortholog	Annotation
			S2R+		Kc		S2R+				Kc				
			Insulin 10'	sSpitz/EGF 10'	Insulin 10'	sSpitz/EGF 10'	Insulin 0' RNAi	Insulin 10' RNAi	EGF 0' RNAi	EGF 10' RNAi	Kc EGF 10' RNAi	Kc EGF RNAi 30'			
Insulin-specific in S2R+ cells															
	InR	Insulin-like receptor						-0.66	-2.96	-0.57	-0.03	-0.18	-0.34	INSR	receptor
	Pten							0.08	-2.66	0.20	0.20	0.06	-0.28	PTEN	phosphatase
	zfh1	Zn finger homeodomain 1						-2.34	-4.75	-2.07	-1.32	2.29	1.20	ZEB1	transcription factor
	CG1908							2.90	-0.86	2.38	-1.34	-0.73	3.58		unknown
	HFA01508							-1.49	1.81	-0.63	1.23	0.00	0.00		no annotation
	CG18754							2.70	1.02	2.13	1.21	0.09	0.07		enzyme
	CG14810							-1.04	2.42	0.43	-0.48	-0.90	0.21		unknown
	TfIIα	Transcription factor IIFalpha						0.72	3.41	-0.91	0.80	1.58	0.60	GTF2F1	general TF
	Akt1							1.09	2.73	0.01	-0.07	0.14	1.62	AKT2	kinase
Insulin-specific in Kc cells															
	HFA00209							-0.99	-4.09	0.15	-5.27	0.00	0.00		no annotation
	CG7115							0.35	0.26	-0.32	-1.82	0.64	-0.06	PPM1L	phosphatase
	CG12602							1.64	-1.12	-1.29	-2.07	1.53	0.08		ion transport
	pk	prickle						-0.94	-1.37	-1.12	2.03	0.86	1.38	LMO6	cytoskeletal
	PNUTS							-1.50	0.48	-0.07	-4.22	-0.49	0.76		unknown
	B4							-0.35	6.01	0.32	0.52	-0.98	-1.35		unknown
	Gap1	GTPase-activating protein 1						1.92	-0.21	4.51	0.01	1.05	0.86	RASA3	GAP/GEF/GTPase
	Tor	Target of rapamycin						-2.26	2.22	0.01	0.30	-0.14	0.09	FRAP1	kinase
Insulin-only (no effects under EGF)															
	gig	gigas						0.43	-1.78	0.21	0.31	-0.80	-0.47	TSC2	GAP/GEF/GTPase
	Tak1	TGF-beta activated kinase 1						0.41	-2.32	-0.29	0.02	0.02	-0.56	MAP3K7	kinase
	CG3008							1.85	0.04	0.21	0.02	0.08	0.18	RIOK3	kinase
	CG30290							0.08	3.04	-0.22	0.93	-0.33	0.34	MDS018	unknown
	HFA19091							2.77	0.47	-0.23	0.21	0.00	0.00		no annotation
	btI	breathless						1.66	0.98	0.69	0.90	-0.50	-0.59	FGFR2	receptor
	Iva	lava lamp						1.04	0.39	1.07	-1.79	-0.36	-0.24	CEP2	cytoskeletal
	CG13819							-0.17	4.82	0.60	0.70	0.13	-0.87		unknown
	rho	rhomboid						-0.75	2.11	0.28	0.25	-0.38	-0.07		enzyme
	CG9468							1.52	1.56	1.41	-0.44	-0.43	0.32	MAN2B1	metabolic
	Vha13	Vacuolar H[+] ATPase G-subunit						-0.24	0.34	2.44	-1.22	0.46	0.56	ATP6V1G2	ion transport
	CycG	Cyclin G						0.85	-1.53	-0.74	-0.19	0.28	-0.64	CCNG2	cell cycle
	PRL-1							3.60	0.24	0.77	0.34	0.32	1.77	PTP4A1	phosphatase
	CG5346							-0.34	-0.64	3.53	0.63	0.64	0.12		unknown
	SerT	Serotonin transporter						0.89	-2.12	0.54	0.76	0.31	0.66	SLC6A4	other
	CG14460							0.94	2.35	0.93	1.06	0.79	-0.92		unknown
EGF-specific in S2R+ cells															
	CG11451							-3.20	-1.71	-0.33	-3.10	0.83	0.21		unknown
	CG6051							-0.17	0.92	0.32	-3.04	-1.46	-0.70		unknown
EGF-specific in Kc cells															
	Hmgcr	HMG Coenzyme A reductase						-1.82	-2.01	-1.79	-3.19	-1.99	-0.29	HMGCR	metabolic
	CG32955							-1.87	-1.18	2.49	0.33	0.11	-0.33	C17orf49	unknown
	CG9339							-0.67	1.59	-1.63	2.52	0.13	0.00	KIAA1171	unknown
	Hsp83	Heat shock protein 83						0.74	1.78	0.74	-1.82	1.63	2.34	HSPCA	chaperone
EGF-only (no effects under insulin)															
	HFA05595							-2.62	1.88	2.01	0.70	0.13	-0.29		no annotation
	RSG7	Regulator of G-protein signaling 7						0.09	0.48	-0.17	1.76	-1.51	-0.70	RGS7	GAP/GEF/GTPase
	CG1796							0.15	2.03	-0.34	0.91	-1.79	0.18	PLRG1	unknown
	unk	unkempt						-0.49	-0.19	0.27	-1.52	-0.05	0.17	ZC3HDC5	transcription factor
	Egfr	Epidermal growth factor receptor						0.34	-0.05	-0.13	-7.69	-5.77	-3.33	EGFR	receptor
	Snap	Soluble NSF attachment protein						-1.18	1.61	-0.83	-3.33	-2.86	-1.99	NAPA	trafficking
	Ptp61F	Protein tyrosine phosphatase 61F						0.61	-0.26	0.41	-1.63	0.38	-0.51	PTPN1	phosphatase
	Chc	Clathrin heavy chain						0.70	0.60	6.13	1.71	0.44	-0.05	CLTC	trafficking
	CG8929							-0.21	0.59	0.37	2.14	-0.39	-1.54		unknown
	ttk	tramtrack						-1.23	-2.69	-1.68	2.40	0.21	0.20	ZNF499	transcription factor
	CG7324							-0.09	-0.43	-0.59	1.65	0.80	-0.17	KIAA0882	GAP/GEF/GTPase

dpERK	%Control
	>125%
	110-125%
	105-110%
	95-105%
	90-95%
	70-90%
	<70%